ELSEVIER

Fusion Engineering and Design 29 (1995) 89–97

Fusion Engineering and Design

Thermomechanical design of the grazing incidence metal mirror of the Prometheus-L IFE reactor

N.M. Ghoniem, A. El-Azab

46-147G Eng. IV, Mechanical, Aerospace and Nuclear Engineering Department, University of California, Los Angeles, CA 90095, USA

Abstract

In laser IFE reactors the reflectivity and absorptivity of the grazing incidence metal mirror (GIMM) depend on the neutron dose received by the mirror surface. In addition to this effect, surface deformation caused by neutron-irradiation-induced swelling and due to thermal load changes the focusing quality of the mirror. In the present work, we present the database for material selection of the final GIMM of the Prometheus-L IFE reactor. A unique design for the GIMM, which accounts for mirror surface deformation by thermal and swelling effects is then presented.

Introduction

The presence of energetic neutrons which stream out of a fusion cavity through the laser ducts makes it difficult to use conventional dielectric mirrors for final focusing purposes. Transmission measurements for conventional dielectrics show that the absorption coefficient of MgF_2 and the optical transmission of ZnS for wavelengths of interest (250–500 mm) degrade by an order of magnitude after 10^{16} n cm^{-2} [1]. This is an extremely low fluence limit, and even if most of the color centers are annealed out by periodic heating, residual defects would still remain and lead to an extremely short lifetime. For these reasons, a metal mirror surface is chosen as the final optical element in the laser system of the Prometheus-L reactor [2].

At each laser pulse, the mirror surface absorbs a certain amount of the laser energy, which leads to instantaneous surface heating. This, in turn, causes surface deformation, which may still exist at the next pulse. Since the surface deformation conditions must be kept to an absolute minimum (fraction of wavelength), the mirror must be designed to accommodate the surface heating, without significant surface deformation. Candidate materials for metal mirrors, such as Al, Mg, Ag, and Cu which exhibit promising optical performance, are susceptible to neutron irradiation to some degree, which may have some limitations on the mirror lifetime. Swelling of these materials under neutron irradiation can be a limiting factor.

In the present work, we present the database which is relevant to materials selection of the final grazing incidence metal mirror (GIMM) of the Prometheus-L reactor. Data on surface reflectivity and absorptivity for laser light are reviewed for some candidate materials. The effects of irradiation on the optical properties and bulk behavior of candidate materials are also presented. The final configuration and design rationale for the GIMM are discussed. In this design, surface deformation of the mirror is minimized by constraining thermal deformation and tailoring the irradiation-induced swelling.

0920-3796/95/$09.50
SSDI 0920-3796(94)00237-1

Table 1
Reflectivities of materials of interest (polished surfaces)

Element		R (%)
C	0.5–10	22–59
Mg	0.5–9	72–93
Al	1–12	71–98
Si	0.5–10	32–28
Fe	0.5–9	55–94
Ag	0.8–9	96.8–98.7

2. Metal reflectivity and absorptivity for laser light

The surface material for the GIMM must have the highest reflectivity and lowest absorptivity. This choice is necessary so that damage to the mirror's surface is minimized. Table 1 gives the room temperature reflectivity for materials of interest. These values are experimental and are for polished surface reflectivity of light of long wavelength (500–10 000 nm) [3].

In the wavelength range of interest (i.e. 200–500 nm), metal reflectivities are strong functions of the wavelength (photon energy) and the angle of incidence. It is desirable to select a material which does not exhibit electronic absorption bands close to the operational regime of KrF laser. Fig. 1 shows the reflectivity of Ag, Al and Mg at normal incidence as a function of the wavelength. The strong photon–electron interaction in Ag for wavelengths in the vicinity of 320 nm would exclude it from our list since the wavelength of the KrF laser is 300 nm. At grazing incidence ($\theta = 85°$), the reflectivities of both Al and Mg markedly improve, as can be seen in Fig. 2. For KrF laser light, the reflectivity of both Al and Mg is about the same (99.4%).

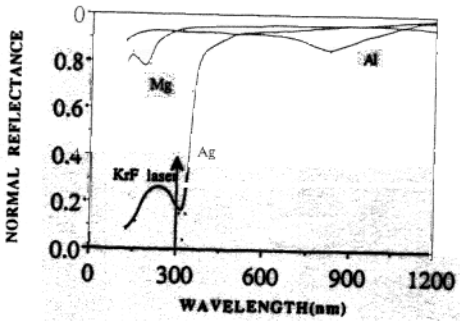

Fig. 1. Reflectivity of Ag, Al, and Mg at normal incidence as a function of wavelength for KrF laser.

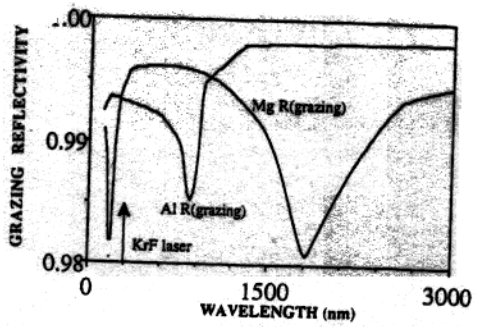

Fig. 2. Grazing reflectivity ($\theta = 85°$) of Al and Mg as a function of wavelength for KrF laser.

3. Radiation effects on candidate materials

Neutron irradiation results in a number of detrimental effects on the mirror's optical performance. Defects, in the form of vacancies, interstitials, transmutations, and subsequent microstructural changes, lead to deterioration of the focusing quality of the mirror and increase the absorption of the incident laser light. In the following, we discuss the salient effects of neutron irradiation and show how such effects can be accommodated in the present design. The two main areas of concern are the effects of produced defects on increasing the electrical resistivity (and hence the laser light absorptivity) of the mirror and the deformation of the mirror's surface, leading to defocusing of the laser beam.

3.1. Radiation effects on resistivity and surface absorptivity

The increase in the resistivity of the aluminum layer will occur by the accumulation of point defects and transmutation products. The rate of increase in the resistivity due to point defects must saturate, either by overlap of neighboring collision cascades or by thermal annealing effects. The rate of resistivity change can be written as

$$\frac{d\rho}{dt} = k\sigma_d \phi \rho_f - \frac{\rho}{\tau} \qquad (1)$$

where k is an efficiency factor, σ_d is the displacement cross-section, ϕ is the neutron flux, ρ_f is the measured resistivity increase per Frenkel pair and τ is the cascade lifetime in aluminum. Eq. (1) shows that the resistivity will saturate at a neutron fluence $(\phi t)_{sat.} = \phi\tau$. At high temperatures, τ is very short, and resistivity saturation will occur at a very small fluence (on the order of

10^{17}–10^{18} n cm^{-2}). At cryogenic temperatures (77 K), the corresponding change in the mirror's absorptivity is reported to be less than 1%, at normal incidence, and less than 0.5% at grazing incidence [3]. In the Prometheus-L design, however, the aluminum surface will run hot, and point defect annealing will result in a further decrease in the magnitude of the irradiation induced absorptivity. The contribution of transmutations to the increase in resistivity, and hence the absorptivity of the surface, does not saturate, as is the case with point defects. However, the resistivity increase per transmutation atom is 4–5 orders of magnitude less than that for point defects [3]. For this reason, their contribution during the mirror's lifetime will be negligible.

Sputtering of surface atoms can lead to roughening. It is experimentally estimated that the sputtering yield of 14 MeV neutrons is on the order of 5×10^{-4} per neutron [4]. If a gas shield is introduced to protect from X-rays, additional sputtering from argon atoms will contribute by a small amount [2], on the order of 6% of the neutron sputtering value. These sputtering events can lead to surface features which would destroy the quality of the laser beam. However, since the aluminum surface temperature will be high, atomic surface diffusion is expected to result in the removal of material layer by layer from the surface of the mirror.

In conclusion, we estimate that the total increase in absorptivity of the mirror due to point defects, transmutations and sputtering is on the order of 0.5%, and that it will saturate after few days of operation under the conditions of the Prometheus-L. For all practical purposes therefore, the reflectivity for 300 nm laser light will degrade to 99% (i.e. only 1% of the light will be absorbed).

3.2. Neutron-induced swelling

When non-uniform swelling takes place in the aluminum layer, gradients in surface displacement will occur. Focusing of the laser light may become impossible if surface undulations on the order of 1.4 of the wavelength result. This tolerance (about 75 nm) is very strict, and has actually resulted in very short lifetimes for similar mirrors in other conceptual designs.

Neutron swelling data on aluminum and magnesium reveal a strong dependence on the impurity level. Experimental data of Adda [4], at 70°C, are summarized in Figs. 3 and 4. The base case for the Prometheus-L designs (99.994% purity) is replotted in Fig. 5, where the swelling is shown as a function of the high energy neutron fluence. It is clear from this figure that alu-

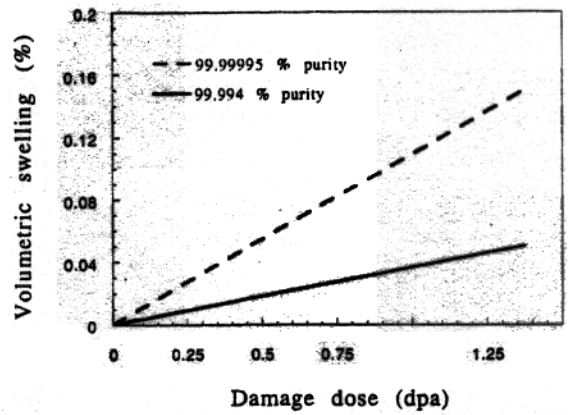

Fig. 3. Neutron-irradiation-induced swelling at 70 °C in Al, as a function of damage dose.

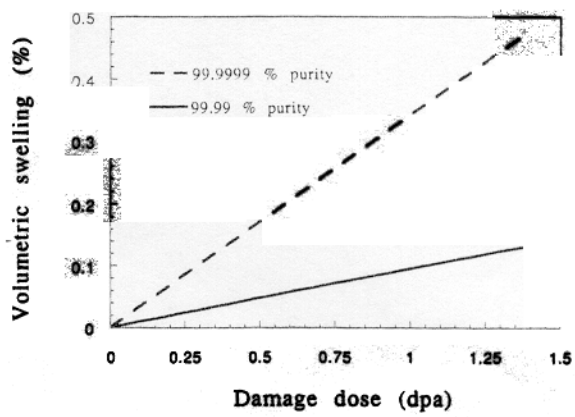

Fig. 4. Neutron-irradiation-induced swelling at 70 °C in Mg, as a function of damage dose.

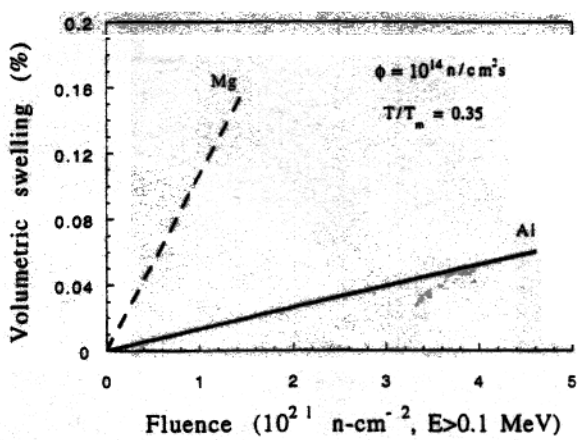

Fig. 5. Projected swelling of Al and Mg under Prometheus-L conditions.

minum will be a better choice for the mirror's surface than magnesium. The following design equation is used to fit the swelling data of aluminum and magnesium:

$$\frac{\Delta V}{V}(\%) = K\phi t \tag{2}$$

where K is a constant and ϕt is the neutron fluence in neutrons per square centimeter. The constant K is found to be 1.29×10^{-21} cm^2 n^{-1} and 1.11×10^{-21} cm^2 n^{-1} for Mg and Al respectively.

4. Design rationale and mirror configuration

The basic design philosophy of the mirror is to separate the functions of each material. For this reason, a high reflectivity aluminum surface is created by a chemical vapor deposition process on top of an SiC structure. The SiC structure is stiffened in two transverse directions by two sets of I-beams. The surface is cooled by flowing helium through the coolant channels. A top view of the mirror is shown in Fig. 6(a). The size of the mirror is dictated by two factors:

(a) maximum temperature rise in the aluminum during the laser pulse should not exceed the recrystallization temperature;
(b) the thermal stress induced in the aluminum layer should not exceed its fatigue endurance limit.

The optical properties of the mirror's surface have been decoupled from the mechanical properties of the supporting structure. In this regard, we have achieved a great degree of flexibility in the design. The surface of the GIMM has been chosen to be metallic, because dielectric materials exhibit great sensitivity to the effects of ionizing radiation. The leading high reflectivity candidate metals are aluminum, magnesium, silver, gold, and copper. To select between these metals, we consider the following criteria.

(1) high reflectivity in the wavelength of interest (i.e. 250–500 nm);
(2) effects of radiation on absorptivity;
(3) surface temperature rise during the laser pulse;
(4) thermal fatigue resistance;
(5) radiation effects on surface deformation.

Although silver has excellent reflectivity, neutron-induced microclusters are expected to distort the mirror's surface. Near-surface collision cascades in silver will be very dense, because of the high electronic stopping power of silver. On the contrary, copper is excluded on the basis of its high neutron-induced swelling, particularly when it is pure. The higher fatigue strength of aluminum results in a smaller mirror size, when it is compared with magnesium. In addition, the neutron-induced swelling rate of commercial grade aluminum is lower than that of magnesium. For the above reasons, aluminum has been chosen as the material for the surface of the mirror.

The structural support of the mirror is composed of two parts: a low swelling composite SiC high rigidity component, and a concrete shell for control of thermal deformations. The SiC structure is designed to have small helium cooling channels, running along the length of the mirror. Two other layers are attached immediately underneath. Each one of these two layers is stiffened by I-beams. The SiC composite is chosen for the following reasons:

(1) very low neutron-induced deformations by thermal and irradiation creep mechanisms in the temperature range 500–700 K;
(2) for porosity of approximately 10%–15%, no neutron swelling is to be expected, and thus mechanical deformations of the mirror's surface are minimized;
(3) SiC is a low activation material, so the choice of SiC will allow passive safety, and shallow land burial of the mirror at the end of life.

In addition to the SiC structure, a concrete shell is designed to provide complete restraint to out-of-plane deformations. This is achieved by sliding bolting mechanisms for the attachment of the bottom of the SiC structure to the concrete shell.

Since the coefficient of thermal expansion of aluminum is higher than that of SiC, a shear graphitic layer is deposited first on the surface of the SiC composite, and the aluminum is added on top of the graphitic shear layer. With this arrangement, in-plane mismatch thermal expansions of the aluminum can be isolated from the SiC composite structure.

The criteria for sizing the mirror will be shown in the next section. A cross-section in the mirror is shown in Fig. 6(b), and the details are illustrated in Fig. 6(c), Thermal expansion gaps are provided around the mirror structure so that buckling is prevented. The main structure of the mirror (SiC) is surrounded by a rigid concrete structure. This support structure is designed to prevent mirror deflections by distributed clamping forces, over a 30 cm distance. The magnitude of the distributed clamping forces will be calculated in the section on surface deformations.

5. Thermal design of the grazing incidence metal mirror

The steady state temperature gradients and the instantaneous rise in the mirror's surface temperature

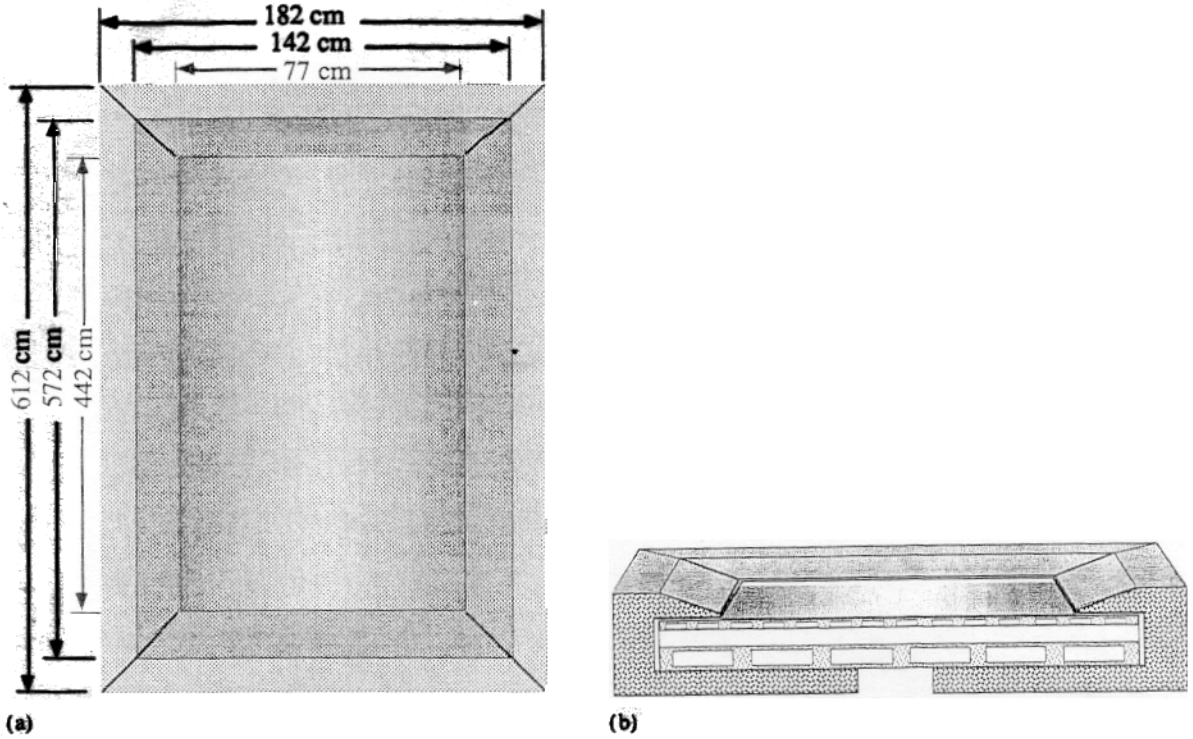

Fig. 6. (a) Top view of the mirror showing dimensions; (b) mirror cross-section; (c) materials and cooling details.

should be minimized by appropriate cooling. A degree of control exists in minimizing the steady state temperature gradients, but the instantaneous surface temperature rise is almost a material property, since the duration of the laser pulse (a few nanoseconds) is much shorter than typical thermal diffusion

times. The optical penetration distance of the laser light is given by

$$d = \frac{\lambda}{4\pi\kappa} \tag{3}$$

where λ is the wavelength, and κ is the extinction coefficient. For a KrF laser on aluminum, this distance is only 7 nm for normal incidence, and about 2–3 atomic layers for grazing incidence. It is concluded, therefore, that a good approximation to the surface temperature will be an instantaneous temperature rise given by

$$\Delta T_s = \frac{2(1 - R_s)q_b}{k}\left(\frac{\alpha_{th} t}{\pi}\right)^{1/2} \tag{4}$$

where q_b is the instantaneous surface power density, t is the duration of the laser pulse, k is the thermal conductivity, α_{th} is the thermal diffusivity and R_s is the reflectivity for the aluminum surface.

The mirror can be designed with convective helium cooling, in the coolant channels shown in Figs. 6(b) and 6(c). Since heat loss from the bottom surface of the mirror to its bottom surface will be slightly greater than across the thickness of the cooling channel, and of convective heat transfer design, are shown in Table 2. The temperature drop across a 2 cm channel wall at the average heat flux can be computed as follows. For a total laser pulse energy of 5 MJ, equally distributed between 60 mirrors each of which has surface area of 77 cm × 442 cm = 2.04×10^6 cm^2, the incidence energy density on the mirror surface is calculated to be 2.45 J cm^{-2}. For 99% reflectivity, the absorbed energy density is 0.01×2.45 J cm^{-2} = 0.0245 J cm^{-2}. The time average heat flux is then calculated as the absorbed energy density per pulse multiplied by the repetition rate. For a repetition rate of 5.65 pulses s^{-1}, the time average surface heat flux is 0.138 425 W cm^{-2}. This average heat flux represents the thermal load to be removed by the helium coolant.

Table 2
Thermal–hydraulic parameters for grazing incidence metal mirror

Parameter	Value	Unit
Wall temperature	450	K
Bulk temperature	350	K
Exit pressure	1	MPa
Pressure drop	19.58	Pa m^{-1}
Bulk velocity	20	m s^{-1}
Reynolds' number	2.47×10^5	
Heat transfer coefficient	261	W m^{-1} K^{-1}

Table 3
Thermophysical properties of high purity aluminum

Parameter	Value	Unit
Thermal conductivity k	2.4	W cm^{-1} K^{-1}
Density ρ	2.7	g cm^{-3}
Specific heat c_p	0.95	J g^{-1} K^{-1}
Thermal diffusivity α	0.936	cm^2 s^{-1}
Characteristic thermal diffusion distance $\langle d \rangle$	0.466	μm
Average energy density $\langle E \rangle$	2.45	J cm^{-2}
Average power density during pulse $\langle q \rangle$	3.6×10^8	W cm^{-2}
Average absorbed power $\langle q \rangle_0$	3.6×10^5	W cm^{-2}
Temperature rise ΔT during pulse	130.6	K

If we take the conductivity of SiC as 0.20 W cm^{-1} K^{-1} (for irradiated SiC at low temperature), then the temperature drop across the support structure will be on the order of 2 K. The effective coolant channel thickness is taken as 4 cm. This small temperature drop must be taken into account for calculations of the thermal deflections of the mirror's surface. When the laser energy is delivered in a short time (7.3 ns), the instantaneous power is very high. When the laser energy is delivered in a short time (7.3 ns), the instantaneous power is very high. The rise in the surface temperature of the mirror is mainly dictated by the thermal diffusivity of the aluminum. Calculations with Eq. (4) give the results shown in Table 3. The instantaneous surface temperature rise is 130.6 K. The corresponding thermal stress can simply be found as

$$\sigma \approx \frac{E}{1 - \nu}\alpha\,\Delta T \tag{5}$$

where α is the coefficient of thermal expansion. Using the properties of annealed aluminum (E = 63.8 GPa, $\alpha = 25 \times 10^{-6}$ °C^{-1}, and ν = 0.34), a thermal stress of 315.6 MPa is calculated, which may exceed the fatigue endurance limit of some aluminum alloys. This limit is in the range 50–390 MPa. However, if we consider radiation hardening effects, the endurance limit can be raised by as much as 50 MPa for aluminum [5].

6. Mechanical deformation of the mirror's surface

The out-of-plane deformation of the mirror's surface should be minimized, or eliminated, if high quality laser

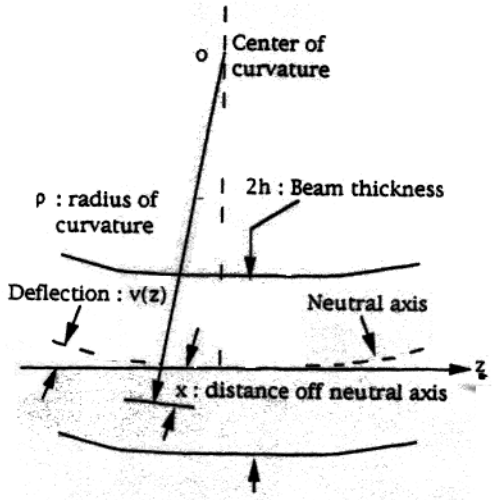

Fig. 7. Illustration of beam deformation theory.

beams are to be maintained. Two main sources of deformation must be analyzed: (1) thermal deformation and (2) neutron-induced swelling deformation. Our design approach is to isolate these two effects. In this respect, we have used an aluminum metal surface and an SiC backing. The temperature of SiC can be kept low enough that neutron-induced swelling is eliminated. We must therefore design for elimination of the deformation of the SiC plate, as a result of the modest temperature difference of a few kelvins. When this is accomplished, the deformation of the aluminum surface by neutron swelling should be compensated for separately. An appropriate theory for calculating the surface deformations would be the theory of plates and shells. However, a good approximation is the elementary beam theory, applied in the two transverse directions. The influence of in-plane shear is neglected in this case.

Consider the elementary theory of straight beams, as illustrated in Fig. 7. The axial strain ε_z is given by

$$\varepsilon_z = \frac{x}{\rho} \tag{6}$$

where x is the distance off the neutral axis, and ρ is the radius of curvature of the mirror's surface. We know, however, that the mirror's curvature is given by

$$\frac{1}{\rho} = \frac{d^2v}{dz^2} \tag{7}$$

where v is the deflection of the mirror's surface, which we try to minimize or, better yet, to eliminate. Combining Eqs. (6) and (7), we obtain a relationship between the strain ε_z and the deflection of the mirror's surface. This is of the form

$$\varepsilon_z = x\frac{d^2v}{dz^2} \tag{8}$$

The total axial strain at any distance x off the neutral axis is composed of an elastic component σ/E and two other inelastic components, the thermal strain component αT, where T is the temperature deviation from the average temperature, and a swelling component ε^s. The latter is equal to one-third of the volumetric swelling. Eq. (8) can be rewritten in the form

$$x\frac{d^2v}{dz^2} = \frac{\sigma}{E} + \alpha T + \varepsilon^s \tag{9}$$

The composite SiC structure is designed to exhibit very low swelling at high temperature, by control of its internal porosity. At low temperature, as is the case in the GIMM, neutron irradiation will produce no swelling. The damaging neutron fluence is estimated from the uncollided neutron flux ϕ_u defined by

$$\phi_u \approx \frac{S_0}{4\pi R_c^2} \tag{10}$$

where R_c is the distance measured from the cavity center, and S_0 is the neutron yield per pulse times the repetition rate. In this approximation, we neglect neutron slowing down and multiple-scattering effects. For example, at the center of the mirror, $\phi_u = 1.957 \times 10^{13}$ n cm^{-2} s^{-1}. With a displacement cross-section of 3140 barns, the flux translates to a defect production rate of $\phi_u\sigma_d \approx 2$ dpa year^{-1}. Detailed neutronics calculations can be very expensive and are probably not warranted at this stage. Such calculations will lead to more accurate results than those given by equation estimated here. However, it is clear that the swelling of SiC will be zero under these conditions, and can, therefore, be eliminated from Eq. (9).

Multiplying both sides of Eq. (9) by bx, where b is the mirror's width, and integrating between $-h$ and $+h$, where $2h$ is the mirror's thickness, we obtain

$$\frac{d^2v}{dz^2} b\int_{-h}^{h} x^2\,dx = \frac{1}{E} b\int_{-h}^{h} x\sigma\,dx + \alpha b\int_{-h}^{h} Tx\,dx \tag{11}$$

Assuming a linear temperature variation across the thickness of the mirror, we obtain

$$T = \frac{\Delta T}{2h}x \tag{12}$$

where ΔT is the temperature difference between the top and bottom surfaces of the mirror. Inserting Eq. (14) into (13) and performing the integrations, we finally obtain the mirror's deflection equation:

$$\frac{d^2v}{dz^2} = \frac{M}{EI} + \frac{\alpha \Delta T}{2h} \tag{13}$$

where M is the acting moment at any specific point in the mirror. We wish here to design the mirror such that $v = 0$ everywhere on the mirror's surface. This can be achieved via Eq. (13) by requiring that

$$\frac{d^2v}{dz^2} = 0 \tag{14}$$

and using clamped end conditions (i.e. $v(0) = v'(0) = v(1) = v'(1) = 0$). The solution to Eq. (13) will yield identically zero deflection everywhere. This situation can be realized in one of the two following ways.

(1) Apply a uniform moment by force couples at distributed locations on the mirror's bottom surface.
(2) Clamp the edges of the mirror to produce a uniform moment everywhere on the mirror's surface. The clamping moment is given by

$$M = -EI\frac{\alpha \Delta T}{2h} \tag{15}$$

We will adopt the second approach in our design here. Clamping forces may be applied either as concentrated force couples or distributed over the mirror edge. The required clamping force P per unit length along the clamp is numerically equal to M/bL, where L is the mirror length, and b is the mirror width. Using the properties of SiC, and a temperature drop of 2 °C (as was shown in the previous section), the magnitude of the clamping force per unit is given by

$$P = \frac{M}{bL} = EI\frac{\alpha \Delta T}{2hbL} \tag{16}$$

7. Neutron-induced swelling of the mirror's surface

Using only the uncollided neutron flux as a first approximation, the displacement rate R in units of dpa per full power year (fpy), at any point on the mirror's surface, which is a distance R_c from the cavity center, is given by

$$R = \phi_u t \sigma_d \tag{17}$$

where ϕ_u is the uncollided flux at R_c. It is interesting to note from the above analysis that the surface deformation will be a function of the thickness of the aluminum layer. Fig. 8 shows the surface deformation at various locations along the mirror's surface. We will analyze the deformation in the following two cases:

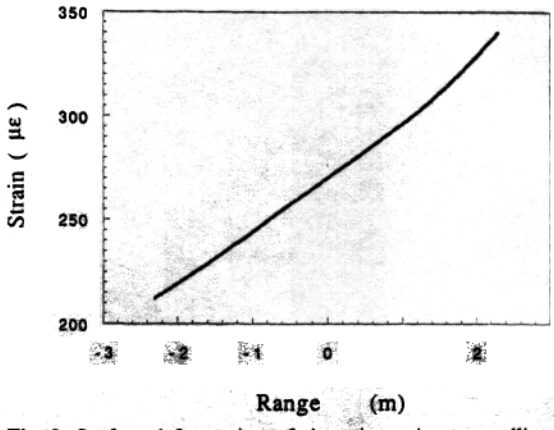

Fig. 8. Surface deformation of the mirror due to swelling.

(1) uniform aluminum layer thickness of 1 mm;
(2) a linear graded thickness of 1 mm at the leading edge of the mirror, to 1.5 mm at the trailing edge.

In the first case, the difference Δ in the normal deformation between the leading and trailing edges is 112 nm, which suggests that the lifetime of the mirror will be about 1 fpy. On the contrary, if the mirror's surface is linearly graded, that difference is given by $\Delta = |332.2 \times 1 - 223 \times 1.5| = 2.3$ nm. It is concluded therefore that the GIMM may last for the plant lifetime, if the present design is adopted.

8. Conclusions

A design database for the GIMM of the Prometheus-L IFE reactor is presented. Two important design issues were discussed: the irradiation effects on the optical performance and deformation of the mirror surface material, and the thermal deformation. Given these two issues a design approach is presented where thermal deformation of the mirror surface is accommodated by using rigid substrates, and the swelling deformation of the surface is accommodated by grading the aluminum thickness to tailor to the swelling deformation. With this design approach, it is shown that the lifetime of GIMM can be reasonably extended.

Acknowledgment

This work was supported by the USDOE Contract DE-AC02-90ER54101.

References

[1] M.J. Weber, Handbook of Laser Science and Technology, Vol. III, Optical Materials, Part 1, CRC, Boca Raton, FL, 1986, pp. 336–366.
[2] M.S. Tillack et al., Initial design of the Prometheus wetted wall IFE reactor cavity, UCLA-FNT-51,1991.
[3] R. Bieri and M. Guinan, An analysis of grazing incidence metal mirrors in a laser ICF reactor cavity, Lawrence Livermore Rep., September 1990.
[4] Y. Adda, Report on the CEA program of investigations of radiation-induced cavities in metals, in Proc. 1971 Int. Conf., Albany, NY, June 1971.
[5] D.S. Billington and J.S. Crawford, Jr., Radiation Damage in Solids, Princeton University Press, Princeton, NJ, 1961.